LA-UR-00-3330

Title: INTEGRATING A LINEAR INTERPOLATION FUNCTION ACROSS TRIANGULAR CELL BOUNDARIES

Author(s) J. Renae Wiseman, U. S. Air Force Academy
Jerry S. Brock, Los Alamos National Laboratory

Submitted: September 2000

Photograph by Chris J. Lindberg

Los Alamos
NATIONAL LABORATORY

Form 836 (10/96)

September 2000 LA-UR-00-3330

Integrating a Linear Interpolation Function Across Triangular Cell Boundaries

J. Renae Wiseman, Mathematics Department
U. S. Air Force Academy, Colorado Springs, CO 80841

Jerry S. Brock, Applied Physics Division
Los Alamos National Laboratory, Los Alamos, NM 87545

Abstract

Computational models of particle dynamics often exchange solution data with discretized continuum-fields using interpolation functions. These particle methods require a series expansion of the interpolation function for two purposes: numerical analysis used to establish the model's consistency and accuracy, and logical-coordinate evaluation used to locate particles within a grid. This report presents *discrete-expansions* for a linear interpolation function commonly used within triangular cell geometries. Discrete-expansions, unlike a Taylor's series, account for interpolation discontinuities across cell boundaries and, therefore, are valid throughout a discretized domain. Verification of linear discrete-expansions is demonstrated on a simple test problem.

Integrating a Linear Interpolation Function Across Triangular Cell Boundaries

Introduction

Particle methods, computational models of particle dynamics, are often solved concurrently with discretized continuum-field equations. Interactive particle methods, including models of liquid sprays, bubble dynamics, and material-interface tracking, strongly couple the governing equations through the bilateral exchange of mass, momentum, and energy. In contrast, reactive particle methods, including models of atmospheric transport, porous-media diffusion, and transient mixing, weakly couple the governing equations; reactive particles simply respond to the entraining continuum field. Another reactive method, used extensively for solution visualization, free-surface tracking, and front tracking, is the tracer-particle method which advects a massless particle with an interpolated velocity. Both interactive and reactive particle methods exchange data with discrete fields using interpolation functions. The focus of this research was on the role of one linear interpolation function commonly used within particle methods.

Particle methods often use interpolation functions directly to evaluate terms in their governing equations. A Taylor's series of the interpolation function, expanded from the particle's cell, is required to perform analytical studies of these numerical methods. The numerical analyses include establishing the model's mathematical consistency and numerical accuracy. The particle's equations, including kinematic equations-of-motion, are often numerically integrated using multi-step methods such as Runge-Kutta methods. The interpolated quantities within the particle's discretized governing equations may be evaluated in a neighboring cell, and the required interpolation expansion would then extend through multiple cells in the grid. Derivatives of interpolation functions, however, are generally not continuous across cell boundaries and, therefore, a Taylor's series is not valid in this situation. An alternative expansion for linear interpolation functions is required to complete numerical analyses for these particle methods.

Particle methods also often use interpolation functions indirectly to evaluate particle-grid connectivity data: the identity of the grid cell in which the particle resides and the particle's logical-coordinate position vector relative to that cell. Particle localization establishes this data using cell-searching and logical-coordinate evaluation methods [1-7]. Cell-searching methods typically use the particle's logical coordinates to both direct and halt the search. Logical-coordinate evaluation involves transforming a physical-space position vector into a local coordinate system, and, as described below, existing methods are based on interpolation expansions. Particle methods, therefore, require interpolation expansions for numerical analysis and localization, and the mathematical expression required for both purposes is identical.

While multi-cell Taylor's series of interpolation functions are generally not valid for numerical analyses, modified versions of these expansions are used for particle localization. For spatial-transformation, the arguments of the interpolation function are logical-coordinate and cell-vertex coordinate vectors. Existing logical-coordinate evaluation methods, generalized in Reference [1] for various cell geometries, were developed from a truncated, single-variable Taylor's series expansion of the interpolation function [1,3,5-7]. The modified Taylor's series avoids discontinuous interpolation derivatives across cell boundaries by ignoring the function's dependence on cell-vertex coordinates. Furthermore, non-linear spatial-transformation problems are linearized by only considering the interpolation function's first-order dependence on logical coordinates. The iterative solution of the resulting system of equations is, however, neither algorithmically robust nor computationally efficient. An alternative expansion for linear interpolation functions is required for robust and efficient particle localization methods.

An alternative type of expansion, a *discrete-expansion*, was recently proposed and validated for multi-linear interpolation functions [8-10]. Discrete-expansions are similar to multi-variable expansions but, unlike a Taylor's series, they are valid throughout a discretized domain. Discrete-expansions are valid for numerical analyses since they acknowledge the full functional dependence of interpolation and account for discontinuous derivatives across cell boundaries. Furthermore, the solution of discrete-expansions for logical-coordinate evaluation is both algorithmically robust and computationally efficient. Using a simple finite-difference technique, a single discrete-expansion was developed for trilinear interpolation defined within three-dimensional hexahedral cells [8,9]. Multiple discrete-expansions were recently developed for bilinear interpolation defined within quadrilateral cells [10]. These two-dimensional discrete-expansions were developed using a general total-differential technique.

This report presents the development of discrete-expansions for linear interpolation defined within two-dimensional triangular cell geometries. This report serves as a companion paper to Reference [10] where the bilinear discrete-expansions were presented. This report will show that the new discrete-expansions are a simplification of the trilinear and bilinear expansions; linear interpolation is more simple than a multi-linear function. The unique formulations of discrete-expansions for linear interpolation, however, will also be identified. This report continues by parametrically integrating the linear interpolation function's total-differential between two particles located in separate, non-contiguous grid cells. Application of the new linear interpolation expansions for numerical analysis or localization within particle methods is beyond the scope of this report. The utility of discrete-expansions for these purposes, however, is outlined and discussed in Reference [10]. A summary concludes this report, and then an appendix presents a test problem, which clearly demonstrates the validity of linear discrete-expansions.

Linear Interpolation

Two-dimensional computational space is frequently discretized into triangular cells, particularly around complex geometries. Linear functions are often applied within these cells for both data interpolation and spatial-transformation. Interpolation produces a continuous mapping of discrete continuum-field data, often located at cell-vertices, to any position within the cell. Spatial transformation includes mapping computational cell geometries from a physical-space, $\bar{X} = (x, y)^T$, to a logical-space, $\bar{\xi} = (\xi, \eta)^T$, coordinate system; see Figure 1. The linear interpolation function is dependent upon both $\bar{\xi}$ and the cell-vertex (cv) coordinate vector, $\bar{X}^{cv} = ({}^0\bar{X}, {}^1\bar{X}, {}^2\bar{X})^T$, as presented in Equation 1.

$$\begin{aligned} \bar{X}(\bar{\xi}, \bar{X}^{cv}) = {} & (1 - \xi - \eta) \, {}^0\bar{X} \\ & + (\quad \xi \quad) \, {}^1\bar{X} \\ & + (\quad \eta \quad) \, {}^2\bar{X} \end{aligned} \tag{1}$$

Equation 1 is linear with respect to both the logical-coordinates, $\bar{\xi}$, and cell-vertex coordinates, $\bar{X}^{cv}$. While the physical coordinates of the triangle's vertices are arbitrary, the transformed coordinates are bound by $\xi \geq 0$, $\eta \geq 0$, and $\xi + \eta \leq 1$. Linear interpolation within one-dimensional line-elements may be obtained from Equation 1 by setting $\eta = 0$.

Total Differential

Using the interpolation function, $\bar{X}(\bar{\xi}, \bar{X}^{cv})$, the objective is to establish a relationship between the finite change of the physical coordinates, $\Delta\bar{X}$, the logical coordinates, $\Delta\bar{\xi}$, and the cell-vertex coordinates, $\Delta\bar{X}^{cv}$. The function's total-differential provides a relationship between infinitesimal changes of these coordinates, $d\bar{X} = f(d\bar{\xi}, d\bar{X}^{cv})$, as presented in Equation 2.

$$d\bar{X} = \frac{\partial \bar{X}(\bar{\xi}, \bar{X}^{cv})}{\partial \bar{\xi}} \, d\bar{\xi} + \frac{\partial \bar{X}(\bar{\xi}, \bar{X}^{cv})}{\partial \bar{X}^{cv}} \, d\bar{X}^{cv} \tag{2}$$

Integration of Equation 2 between two particle end-states will provide the relationship $\Delta\bar{X} = f(\Delta\bar{\xi}, \Delta\bar{X}^{cv})$, which functionally represents a discrete-expansion for interpolation.

Logical Coordinate Derivative

The linear interpolation function's total-differential includes two first-order derivatives or transformation matrices that are scaled by differential-coordinate vectors. The first derivative in Equation 2 represents a coordinate-transformation or Jacobian matrix, $J = \partial\bar{X}/\partial\bar{\xi}$. The Jacobian matrix's square structure is defined in Equation 3 for a two-dimensional transformation.

$$\left[\frac{\partial \bar{X}}{\partial \bar{\xi}}\right]_{2x2} = \left[\frac{\partial \bar{X}}{\partial \xi} \quad \frac{\partial \bar{X}}{\partial \eta}\right]_{2x2} = \begin{bmatrix} \frac{\partial x}{\partial \xi} & \frac{\partial x}{\partial \eta} \\ \frac{\partial y}{\partial \xi} & \frac{\partial y}{\partial \eta} \end{bmatrix}_{2x2} \tag{3}$$

The size of the Jacobian matrix is determined by the number of spatial dimensions. Elements of the coordinate-transformation matrix are most easily defined using column vectors. For two-dimensional linear interpolation, these derivatives are presented in Equation 4.

$$\begin{aligned} \frac{\partial \bar{X}}{\partial \xi}(\bar{X}^{cv}) &= {}^{1}\bar{X} - {}^{0}\bar{X} \\ \frac{\partial \bar{X}}{\partial \eta}(\bar{X}^{cv}) &= {}^{2}\bar{X} - {}^{0}\bar{X} \end{aligned} \tag{4}$$

Each derivative within Equation 4 is a linear function of the cell-vertex coordinates. The Jacobian matrix for two-dimensional linear interpolation, which combines these column vectors, is, therefore, a linear function with respect to $\bar{X}^{cv}$: $J = \partial \bar{X}(\bar{X}^{cv})/\partial \bar{\xi}$.

Cell-Vertex Coordinate Derivative

The second derivative in the linear interpolation function's total-differential, Equation 2, represents a geometry-transformation matrix. The matrix structure of $\partial \bar{X}/\partial \bar{X}^{cv}$, the cell-vertex coordinate derivative, is defined in Equation 5 for triangular cell geometries.

$$\left[\frac{\partial \bar{X}}{\partial \bar{X}^{cv}}\right]_{2x6} = \left[\frac{\partial \bar{X}}{\partial {}^{0}\bar{X}} \quad \frac{\partial \bar{X}}{\partial {}^{1}\bar{X}} \quad \frac{\partial \bar{X}}{\partial {}^{2}\bar{X}}\right]_{2x6} \tag{5}$$

The number of rows and columns in the non-square geometry-transformation matrix are determined by the problem dimension size and the number of elements within the cell-vertex coordinate vector, $\bar{X}^{cv}$. The size of $\bar{X}^{cv}$ is equal to the number of spatial dimensions multiplied by the number of cell vertices. The geometry-transformation matrix may be partitioned into sub-matrices, which are each associated with a cell-vertex position 'v' as presented in Equation 6.

$$\left[\frac{\partial \bar{X}}{\partial {}^{v}\bar{X}}\right]_{2x2} = \left[\frac{\partial \bar{X}}{\partial {}^{v}x} \quad \frac{\partial \bar{X}}{\partial {}^{v}y}\right]_{2x2} = \begin{bmatrix} \frac{\partial x}{\partial {}^{v}x} & \frac{\partial x}{\partial {}^{v}y} \\ \frac{\partial y}{\partial {}^{v}x} & \frac{\partial y}{\partial {}^{v}y} \end{bmatrix}_{2x2} \tag{6}$$

The square structure and size of each partition within the geometry-transformation matrix are similar to the Jacobian matrix, Equation 3. In contrast to the full Jacobian matrix, however, each of the sub-matrices within $\partial\bar{X}/\partial\bar{X}^{cv}$ are diagonal as presented in Equation 7.

$$\left[\frac{\partial\bar{X}}{\partial^{v}\bar{X}}\right]_{2x2} = \begin{bmatrix} \frac{\partial x}{\partial^{v}x} & 0 \\ 0 & \frac{\partial y}{\partial^{v}y} \end{bmatrix}_{2x2} \tag{7}$$

The non-zero elements of the sub-matrices within $\partial\bar{X}/\partial\bar{X}^{cv}$ are most easily defined for each cell-vertex position. These elements, $\partial x/\partial^{v}x$ and $\partial y/\partial^{v}y$, are the basis functions used within the two-dimensional linear interpolation function as presented in Equation 8.

$$\begin{aligned} \frac{\partial x}{\partial^{0}x}(\bar{\xi}) &= \frac{\partial y}{\partial^{0}y}(\bar{\xi}) = (1 - \xi - \eta) \\ \frac{\partial x}{\partial^{1}x}(\bar{\xi}) &= \frac{\partial y}{\partial^{1}y}(\bar{\xi}) = (\xi) \\ \frac{\partial x}{\partial^{2}x}(\bar{\xi}) &= \frac{\partial y}{\partial^{2}y}(\bar{\xi}) = (\eta) \end{aligned} \tag{8}$$

For each cell-vertex position, the non-zero derivatives are identical: $\partial x/\partial^{v}x = \partial y/\partial^{v}y$. Each sub-matrix may then be defined as an identity matrix scaled by an interpolation basis function. The derivatives within Equation 8 are linear functions of the logical-coordinates. The geometry-transformation matrix for two-dimensional linear interpolation, which combines these column vectors, is, therefore, a linear function with respect to $\bar{\xi}$: $\partial\bar{X}(\bar{\xi})/\partial\bar{X}^{cv}$.

Since linear interpolation is linear with respect to both $\bar{\xi}$ and $\bar{X}^{cv}$, the transformation matrices, first-order derivatives, are functions of only one variable; the coordinate-transformation matrix is only a function of $\bar{X}^{cv}$ and the geometry-transformation matrix is only a function of $\bar{\xi}$. The linear interpolation function's simplified total-differential is presented in Equation 9.

$$d\bar{X} = \frac{\partial\bar{X}}{\partial\bar{\xi}}(\bar{X}^{cv})\, d\bar{\xi} + \frac{\partial\bar{X}}{\partial\bar{X}^{cv}}(\bar{\xi})\, d\bar{X}^{cv} \tag{9}$$

Integration Method

The objective is to integrate the linear function's total-differential, Equation 9, to obtain a discrete-expansion for interpolation: $\Delta\bar{X} = f(\Delta\bar{\xi}, \Delta\bar{X}^{cv})$. The integration limits are two particles

located in separate grid cells: State 1, $\bar{X}_1 = \bar{X}(\bar{\xi}_1, \bar{X}_1^{cv})$, and State 2, $\bar{X}_2 = \bar{X}(\bar{\xi}_2, \bar{X}_2^{cv})$. The computational sub-domains in which the particles reside are not desired to be connected in physical-space. Integration of the total-differential is represented in Equation 10.

$$\int_1^2 d\bar{X} = \int_1^2 \frac{\partial \bar{X}}{\partial \bar{\xi}}(\bar{X}^{cv})\, d\bar{\xi} + \int_1^2 \frac{\partial \bar{X}}{\partial \bar{X}^{cv}}(\bar{\xi})\, d\bar{X}^{cv} \tag{10}$$

The linearity and continuity of the derivatives in the total-differential affect the integration process used to obtain a discrete-expansion. The linearity of the interpolation derivatives determines the complexity of the integration process. For linear interpolation, the coordinate-transformation and geometry-transformation matrices are linear with respect to $\bar{\xi}$ or $\bar{X}^{cv}$. More importantly, continuity of the interpolation derivatives is required for the total-differential to be valid within a specified region. Solution of Equation 10 in a single cell is straightforward; the interpolation derivatives are guaranteed to be continuous in this region. In contrast, if the limits of integration cross a cell boundary, solution of Equation 10 is more complex.

Solution of Equation 10 between particles located in separate but adjoining cells involves integrating the total-differential through two unique coordinate systems. While the form of the interpolation expression is identical for each cell, the two functions are different; they have distinct cell-vertex coordinate vectors. Along their common cell-edge, linear interpolation functions are continuous but their derivatives are generally discontinuous. Direct integration of the total-differential is, therefore, not possible along any pathline that crosses a cell boundary. Discrete-expansions may be obtained from Equation 10 if the integration pathline is partitioned or if the integration coordinate-space is appropriately parameterized.

An integration pathline that passes between adjoining cells may be partitioned into two line-segments, each defined within a separate coordinate system. The integrals within Equation 10 are similarly partitioned into cell-based segments along which the interpolation derivatives are guaranteed to be continuous. Integration along this two-segment pathline would proceed within the first cell from State 1 to the common cell edge, then within the second cell to State 2. While this procedure represents a valid method of solution for Equation 10, it is algorithmically complex and computationally expensive. Furthermore, if the particle end-states are located within non-contiguous grid cells, this solution method is prohibitively complex and expensive.

Parameterization

Alternatively, the coordinate-space between the limits of integration can be parameterized. Parameterization removes the concept of multiple coordinate systems and, thus, discontinuous

interpolation derivatives across cell boundaries, by creating a single coordinate-space between two particles. The integration end-states can then be defined within any two cells, including non-contiguous cells. While the form of the parameterization function is arbitrary, it must be differentiable; it is embedded within the parameterized interpolation function. Derivatives of the parameterized interpolation function are then guaranteed to be continuous. The parameterized total-differential, therefore, may be integrated without requiring a partitioned pathline.

To create a single coordinate-space between two particles, each of the physical, logical, and cell-vertex coordinates must be parameterized; particle states are a collection of these vectors. A simple linear technique using the variable 's', where $0 \le s \le 1$, was selected in this research. The parameterized coordinates, $\overline{X}(s)$, $\overline{\xi}(s)$ and $\overline{X}^{cv}(s)$, then vary linearly along any integration pathline. Integration limits for the parameterized total-differential are the bounding limits of the variable 's'. Integration of the parameterized total-differential is represented in Equation 11.

$$\int_0^1 \frac{\partial \overline{X}(s)}{\partial s}\, ds = \int_0^1 \frac{\partial \overline{X}}{\partial \overline{\xi}}(\overline{X}^{cv}(s))\, \frac{\partial \overline{\xi}(s)}{\partial s}\, ds + \int_0^1 \frac{\partial \overline{X}}{\partial \overline{X}^{cv}}(\overline{\xi}(s))\, \frac{\partial \overline{X}^{cv}(s)}{\partial s}\, ds \qquad (11)$$

Solution of Equation 11 requires an integration pathline defined between the particle States 1 and 2. The only restriction on the limits of integration are that the end-state variables form a consistent set of coordinates as described by the interpolation function: $\overline{X} = \overline{X}(\overline{\xi}, \overline{X}^{cv})$. The integration pathline for the parameterized total-differential traverses through the $(\overline{\xi}, \overline{X}^{cv})$ plane since these vectors are the arguments of the spatial-transformation function. The parameterization function, however, does not prescribe the shape of the integration pathline. Three pathlines, commonly used for parameterized integration problems, were selected by this research to solve Equation 11: direct, upper-step, and lower-step integration pathlines.

Direct Integration Pathline

The first integration pathline used to solve Equation 11 is a straight or direct line between particle States 1 and 2; see Figure 2. The parameterized coordinates, which reduce to the particle end-state coordinates at the bounding limits of integration, are presented in Equation 12.

$$\begin{aligned} \text{State 1} \rightarrow \text{State 2} \quad : \quad \overline{X}(s) &= (1-s)\, \overline{X}_1 + (s)\, \overline{X}_2 \\ \overline{\xi}(s) &= (1-s)\, \overline{\xi}_1 + (s)\, \overline{\xi}_2 \\ \overline{X}^{cv}(s) &= (1-s)\, \overline{X}_1^{cv} + (s)\, \overline{X}_2^{cv} \end{aligned} \qquad (12)$$

Solution of Equation 11 along the direct integration pathline is represented in Equation 13, where the interpolation derivatives are appropriately labeled.

$$\int_0^1 \left.\frac{\partial \bar{X}(s)}{\partial s}\right|_{1\to 2} ds = \int_0^1 \left.\frac{\partial \bar{X}}{\partial \bar{\xi}}(\bar{X}^{cv}(s))\right|_{1\to 2} \left.\frac{\partial \bar{\xi}(s)}{\partial s}\right|_{1\to 2} ds + \int_0^1 \left.\frac{\partial \bar{X}}{\partial \bar{X}^{cv}}(\bar{\xi}(s))\right|_{1\to 2} \left.\frac{\partial \bar{X}^{cv}(s)}{\partial s}\right|_{1\to 2} ds \tag{13}$$

Since the parameterized coordinates are linear functions, their derivatives are constant finite-difference vectors: $\partial \bar{X}(s)/\partial s = \Delta \bar{X}$, $\partial \bar{\xi}(s)/\partial s = \Delta \bar{\xi}$, and $\partial \bar{X}^{cv}(s)/\partial s = \Delta \bar{X}^{cv}$. These difference vectors are defined between particle States 1 and 2: $\Delta \bar{X} = \bar{X}_2 - \bar{X}_1$, $\Delta \bar{\xi} = \bar{\xi}_2 - \bar{\xi}_1$, and $\Delta \bar{X}^{cv} = \bar{X}_2^{cv} - \bar{X}_1^{cv}$. Integration of the parameterized total-differential along the direct pathline can then be simplified as presented in Equation 14.

$$\int_0^1 \Delta \bar{X}\, ds = \int_0^1 \left.\frac{\partial \bar{X}}{\partial \bar{\xi}}(\bar{X}^{cv}(s))\right|_{1\to 2} \Delta \bar{\xi}\, ds + \int_0^1 \left.\frac{\partial \bar{X}}{\partial \bar{X}^{cv}}(\bar{\xi}(s))\right|_{1\to 2} \Delta \bar{X}^{cv}\, ds \tag{14}$$

The parameterized transformation matrices within Equation 14 are formed by substituting $\bar{\xi}(s)$ and $\bar{X}^{cv}(s)$ from Equation 12 into Equations 4 and 8. Solution of Equation 14 is then straightforward, and many expansions may be obtained. The three discrete-expansions most easily obtained using the direct integration pathline are presented in Equation 15.

$$\begin{aligned}
\Delta \bar{X} &= \frac{\partial \bar{X}}{\partial \bar{\xi}}(\hat{\bar{X}}^{cv})\, \Delta \bar{\xi} + \frac{\partial \bar{X}}{\partial \bar{X}^{cv}}(\hat{\bar{\xi}})\, \Delta \bar{X}^{cv} \\
\Delta \bar{X} &= \frac{\partial \bar{X}}{\partial \bar{\xi}}(\bar{X}_1^{cv})\, \Delta \bar{\xi} + \frac{\partial \bar{X}}{\partial \bar{\xi}}(\Delta \bar{X}^{cv})\, \Delta \bar{\xi} + \frac{\partial \bar{X}}{\partial \bar{X}^{cv}}(\bar{\xi}_1)\, \Delta \bar{X}^{cv} \\
\Delta \bar{X} &= \frac{\partial \bar{X}}{\partial \bar{\xi}}(\bar{X}_2^{cv})\, \Delta \bar{\xi} - \frac{\partial \bar{X}}{\partial \bar{\xi}}(\Delta \bar{X}^{cv})\, \Delta \bar{\xi} + \frac{\partial \bar{X}}{\partial \bar{X}^{cv}}(\bar{\xi}_2)\, \Delta \bar{X}^{cv}
\end{aligned} \tag{15}$$

The linear discrete-expansions in Equation 15 are similar to a Taylor's series of a linear function: they are combinations of first-order interpolation derivatives scaled by $\Delta \bar{\xi}$ and $\Delta \bar{X}^{cv}$. Arguments for the transformation matrices are either particle end-state coordinates, coordinate differences, or coordinate averages: $\hat{\bar{\xi}} = (\bar{\xi}_1 + \bar{\xi}_2)/2$ and $\hat{\bar{X}}^{cv} = (\bar{X}_1^{cv} + \bar{X}_2^{cv})/2$.

Upper-Step Integration Pathline

The second integration pathline used to solve Equation 11 is comprised of two line-segments that form an upper-step within the $(\bar{\xi}, \bar{X}^{cv})$ plane. The first pathline segment is a line of constant $\bar{\xi}$ from State 1 to State A; see Figure 2. The second pathline segment is a line of constant $\bar{X}^{cv}$ from State A to State 2. The parameterized coordinates are presented in Equations 16 and 17.

$$
\begin{aligned}
\text{State 1} \rightarrow \text{State A} \quad : \quad \bar{X}(s) &= (1-s)\,\bar{X}_1 + (s)\,\bar{X}_A \\
\bar{\xi}(s) &= (1-s)\,\bar{\xi}_1 + (s)\,\bar{\xi}_A \;;\; \bar{\xi}_A = \bar{\xi}_1 \\
&= \bar{\xi}_1 \\
\bar{X}^{cv}(s) &= (1-s)\,\bar{X}_1^{cv} + (s)\,\bar{X}_A^{cv} \;;\; \bar{X}_A^{cv} = \bar{X}_2^{cv} \\
&= (1-s)\,\bar{X}_1^{cv} + (s)\,\bar{X}_2^{cv}
\end{aligned}
\tag{16}
$$

$$
\begin{aligned}
\text{State A} \rightarrow \text{State 2} \quad : \quad \bar{X}(s) &= (1-s)\,\bar{X}_A + (s)\,\bar{X}_2 \\
\bar{\xi}(s) &= (1-s)\,\bar{\xi}_A + (s)\,\bar{\xi}_2 \;;\; \bar{\xi}_A = \bar{\xi}_1 \\
&= (1-s)\,\bar{\xi}_1 + (s)\,\bar{\xi}_2 \\
\bar{X}^{cv}(s) &= (1-s)\,\bar{X}_A^{cv} + (s)\,\bar{X}_2^{cv} \;;\; \bar{X}_A^{cv} = \bar{X}_2^{cv} \\
&= \bar{X}_2^{cv}
\end{aligned}
\tag{17}
$$

The upper-step integration pathline does not constitute cell-based partition of the original, non-parameterized total-differential. Integration of Equation 10, however, can be rewritten to simulate the upper-step integration pathline as presented in Equation 18.

$$
\begin{aligned}
\int_1^A d\bar{X} + \int_A^2 d\bar{X} &= \int_1^A \frac{\partial \bar{X}}{\partial \bar{\xi}}(\bar{X}^{cv})\, d\bar{\xi} + \int_A^2 \frac{\partial \bar{X}}{\partial \bar{\xi}}(\bar{X}^{cv})\, d\bar{\xi} \\
&+ \int_1^A \frac{\partial \bar{X}}{\partial \bar{X}^{cv}}(\bar{\xi})\, d\bar{X}^{cv} + \int_A^2 \frac{\partial \bar{X}}{\partial \bar{X}^{cv}}(\bar{\xi})\, d\bar{X}^{cv}
\end{aligned}
\tag{18}
$$

Parameterization of Equation 18, the upper-step integration pathline, is represented in Equation 19, where the interpolation derivatives are appropriately labeled.

$$
\begin{aligned}
&\int_0^1 \left.\frac{\partial \bar{X}(s)}{\partial s}\right|_{1\rightarrow A} ds + \int_0^1 \left.\frac{\partial \bar{X}(s)}{\partial s}\right|_{A\rightarrow 2} ds = \\
&+ \int_0^1 \left.\frac{\partial \bar{X}}{\partial \bar{\xi}}(\bar{X}^{cv}(s))\right|_{1\rightarrow A} \left.\frac{\partial \bar{\xi}(s)}{\partial s}\right|_{1\rightarrow A} ds + \int_0^1 \left.\frac{\partial \bar{X}}{\partial \bar{\xi}}(\bar{X}^{cv}(s))\right|_{A\rightarrow 2} \left.\frac{\partial \bar{\xi}(s)}{\partial s}\right|_{A\rightarrow 2} ds \\
&+ \int_0^1 \left.\frac{\partial \bar{X}}{\partial \bar{X}^{cv}}(\bar{\xi}(s))\right|_{1\rightarrow A} \left.\frac{\partial \bar{X}^{cv}(s)}{\partial s}\right|_{1\rightarrow A} ds + \int_0^1 \left.\frac{\partial \bar{X}}{\partial \bar{X}^{cv}}(\bar{\xi}(s))\right|_{A\rightarrow 2} \left.\frac{\partial \bar{X}^{cv}(s)}{\partial s}\right|_{A\rightarrow 2} ds
\end{aligned}
\tag{19}
$$

Along the first segment of the upper-step integration pathline from State 1 to State A, where $\bar{\xi}$ is constant, $\partial\bar{\xi}(s)/\partial s = 0$ and $\partial\bar{X}^{cv}(s)/\partial s = \Delta\bar{X}^{cv}$. Along the second pathline segment from State A to State 2, where $\bar{X}^{cv}$ is constant, $\partial\bar{\xi}(s)/\partial s = \Delta\bar{\xi}$ and $\partial\bar{X}^{cv}(s)/\partial s = 0$.

Along the entire upper-step pathline $\partial\bar{X}(s)/\partial s = \Delta\bar{X}$. Integration of the parameterized total-differential along the upper-step pathline can then be simplified as presented in Equation 20.

$$\int_0^1 \Delta\bar{X}\, ds = \int_0^1 \frac{\partial\bar{X}}{\partial\bar{\xi}}(\bar{X}^{cv}(s))\bigg|_{A\to 2} \Delta\bar{\xi}\, ds + \int_0^1 \frac{\partial\bar{X}}{\partial\bar{X}^{cv}}(\bar{\xi}(s))\bigg|_{1\to A} \Delta\bar{X}^{cv}\, ds \tag{20}$$

The parameterized transformation matrices in Equation 20 are formed by substituting $\bar{\xi}(s)$ and $\bar{X}^{cv}(s)$ from Equations 16 and 17 into Equations 4 and 8. Solution of Equation 20 is then straightforward, and many expansions may be obtained. The single discrete-expansion most easily obtained using the upper-step integration pathline is presented in Equation 21.

$$\Delta\bar{X} = \frac{\partial\bar{X}}{\partial\bar{\xi}}(\bar{X}_2^{cv})\,\Delta\bar{\xi} + \frac{\partial\bar{X}}{\partial\bar{X}^{cv}}(\bar{\xi}_1)\,\Delta\bar{X}^{cv} \tag{21}$$

Within Equation 21, $\partial\bar{X}/\partial\bar{\xi}$ is evaluated at $\bar{X}_2^{cv}$; the logical-coordinates vary along the pathline segment where $\bar{X}^{cv}$ is fixed at State 2. Similarly, $\partial\bar{X}/\partial\bar{X}^{cv}$ is evaluated at $\bar{\xi}_1$; the cell-vertex coordinates vary along the pathline segment where $\bar{\xi}$ is fixed at State 1.

Lower-Step Integration Pathline

The third integration pathline used to solve Equation 11 is comprised of two line-segments that form a lower-step within the $(\bar{\xi}, \bar{X}^{cv})$ plane. The first pathline segment is a line of constant $\bar{X}^{cv}$ from State 1 to State B; see Figure 2. The second pathline segment is a line of constant $\bar{\xi}$ from State B to State 2. The parameterized coordinates are presented in Equations 22 and 23.

$$\begin{aligned}
\text{State 1} \to \text{State B} \quad : \quad \bar{X}(s) &= (1-s)\,\bar{X}_1 + (s)\,\bar{X}_B \\
\bar{\xi}(s) &= (1-s)\,\bar{\xi}_1 + (s)\,\bar{\xi}_B \;;\; \bar{\xi}_B = \bar{\xi}_2 \\
&= (1-s)\,\bar{\xi}_1 + (s)\,\bar{\xi}_2 \\
\bar{X}^{cv}(s) &= (1-s)\,\bar{X}_1^{cv} + (s)\,\bar{X}_B^{cv} \;;\; \bar{X}_B^{cv} = \bar{X}_1^{cv} \\
&= \bar{X}_1^{cv}
\end{aligned} \tag{22}$$

$$\begin{aligned}
\text{State B} \to \text{State 2} \quad : \quad \bar{X}(s) &= (1-s)\,\bar{X}_B + (s)\,\bar{X}_2 \\
\bar{\xi}(s) &= (1-s)\,\bar{\xi}_B + (s)\,\bar{\xi}_2 \;;\; \bar{\xi}_B = \bar{\xi}_2 \\
&= \bar{\xi}_2 \\
\bar{X}^{cv}(s) &= (1-s)\,\bar{X}_B^{cv} + (s)\,\bar{X}_2^{cv} \;;\; \bar{X}_B^{cv} = \bar{X}_1^{cv} \\
&= (1-s)\,\bar{X}_1^{cv} + (s)\,\bar{X}_2^{cv}
\end{aligned} \tag{23}$$

Integration of the non-parameterized total-differential, Equation 10, can be rewritten to simulate the lower-step integration pathline as presented in Equation 24.

$$\begin{aligned}\int_1^B d\bar{X} + \int_B^2 d\bar{X} &= \int_1^B \frac{\partial \bar{X}}{\partial \bar{\xi}}(\bar{X}^{cv})\, d\bar{\xi} + \int_B^2 \frac{\partial \bar{X}}{\partial \bar{\xi}}(\bar{X}^{cv})\, d\bar{\xi} \\ &+ \int_1^B \frac{\partial \bar{X}}{\partial \bar{X}^{cv}}(\bar{\xi})\, d\bar{X}^{cv} + \int_B^2 \frac{\partial \bar{X}}{\partial \bar{X}^{cv}}(\bar{\xi})\, d\bar{X}^{cv}\end{aligned} \tag{24}$$

Parameterization of Equation 24, the lower-step integration pathline, is represented in Equation 25, where the interpolation derivatives are appropriately labeled.

$$\begin{aligned}&\int_0^1 \left.\frac{\partial \bar{X}(s)}{\partial s}\right|_{1\to B} ds + \int_0^1 \left.\frac{\partial \bar{X}(s)}{\partial s}\right|_{B\to 2} ds = \\ &+ \int_0^1 \left.\frac{\partial \bar{X}}{\partial \bar{\xi}}(\bar{X}^{cv}(s))\right|_{1\to B} \left.\frac{\partial \bar{\xi}(s)}{\partial s}\right|_{1\to B} ds + \int_0^1 \left.\frac{\partial \bar{X}}{\partial \bar{\xi}}(\bar{X}^{cv}(s))\right|_{B\to 2} \left.\frac{\partial \bar{\xi}(s)}{\partial s}\right|_{B\to 2} ds \\ &+ \int_0^1 \left.\frac{\partial \bar{X}}{\partial \bar{X}^{cv}}(\bar{\xi}(s))\right|_{1\to B} \left.\frac{\partial \bar{X}^{cv}(s)}{\partial s}\right|_{1\to B} ds + \int_0^1 \left.\frac{\partial \bar{X}}{\partial \bar{X}^{cv}}(\bar{\xi}(s))\right|_{B\to 2} \left.\frac{\partial \bar{X}^{cv}(s)}{\partial s}\right|_{B\to 2} ds\end{aligned} \tag{25}$$

Along the first segment of the lower-step integration pathline from State 1 to State B, where $\bar{X}^{cv}$ is constant, $\partial\bar{\xi}(s)/\partial s = \Delta\bar{\xi}$ and $\partial\bar{X}^{cv}(s)/\partial s = 0$. Along the second pathline segment from State B to State 2, where $\bar{\xi}$ is constant, $\partial\bar{\xi}(s)/\partial s = 0$ and $\partial\bar{X}^{cv}(s)/\partial s = \Delta\bar{X}^{cv}$. Along the entire lower-step pathline $\partial\bar{X}(s)/\partial s = \Delta\bar{X}$. Integration of the parameterized total-differential along the lower-step pathline can then be simplified as presented in Equation 26.

$$\int_0^1 \Delta\bar{X}\, ds = \int_0^1 \left.\frac{\partial \bar{X}}{\partial \bar{\xi}}(\bar{X}^{cv}(s))\right|_{1\to B} \Delta\bar{\xi}\, ds + \int_0^1 \left.\frac{\partial \bar{X}}{\partial \bar{X}^{cv}}(\bar{\xi}(s))\right|_{B\to 2} \Delta\bar{X}^{cv}\, ds \tag{26}$$

The parameterized transformation matrices in Equation 26 are formed by substituting $\bar{\xi}(s)$ and $\bar{X}^{cv}(s)$ from Equations 22 and 23 into Equations 4 and 8. Solution of Equation 26 is then straightforward, and many expansions may be obtained. The single discrete-expansion most easily obtained using the lower-step integration pathline is presented in Equation 27.

$$\Delta\bar{X} = \frac{\partial \bar{X}}{\partial \bar{\xi}}(\bar{X}_1^{cv})\, \Delta\bar{\xi} + \frac{\partial \bar{X}}{\partial \bar{X}^{cv}}(\bar{\xi}_2)\, \Delta\bar{X}^{cv} \tag{27}$$

The lower-step discrete-expansion, Equation 27, is similar to the upper-step expansion, Equation 21. While the form of these discrete-expansions is identical, their interpolation

derivatives are evaluated at opposite particle end-states; the upper-step and lower-step integration pathlines are mirror images of each other. Within Equation 27, the coordinate-transformation matrix is evaluated at $\overline{X}_1^{cv}$ and the geometry-transformation matrix is evaluated at $\bar{\xi}_2$.

The discrete-expansions in Equations 15, 21, and 27, developed for linear interpolation defined in triangular cells, are a simplification of the trilinear [8,9] and bilinear expansions [10]; linear interpolation is more simple than a multi-linear function. Furthermore, the upper-step discrete-expansion within Equation 21 is the linear version of the trilinear expansion which was obtained using the finite-difference method. The total-differential and finite-difference methods, therefore, produce identical discrete-expansions for similar interpolation functions. Finally, a truncated, single-variable Taylor's series expansion of linear interpolation may be obtained if $\overline{X}_2^{cv} = \overline{X}_1^{cv}$ is substituted within any of the above multi-variable discrete-expansions.

However, unique discrete-expansion formulations are possible for linear interpolation; the transformation matrices are easily manipulated since they are linear functions of $\bar{\xi}$ and $\overline{X}^{cv}$. Two expansions in Equation 15 include transformation matrices that are evaluated at the identical particle end-state. A second Jacobian matrix, evaluated with $\Delta\overline{X}^{cv}$, also appears in these expansions. The form of these two expansions is not repeated in the multi-linear solutions. Furthermore, these direct-pathline expansions are related to the other linear discrete-expansions; they are equivalent to the upper-step and lower-step expansions in Equations 21 and 27.

Summary

Five discrete-expansions were developed for linear interpolation defined within two-dimensional triangular cells. Discrete-expansions are similar to multi-variable expansions, but unlike a Taylor's series, they are valid throughout a discretized domain; they account for interpolation discontinuities across cell boundaries. The new expansions were developed by parametrically integrating the interpolation function's total-differential between two particles located in separate, non-contiguous cells. The linear-interpolation expansions are a simplification of multi-linear discrete-expansions, but they exhibit unique formulations. Finally, discrete-expansions can be simplified to obtain a truncated, single-variable Taylor's series expansion.

Acknowledgement

This work was sponsored by the Accelerated Strategic Computing Initiative Program at the Los Alamos National Laboratory. Thanks to Forrest B. Brown, John H. Hall and Stephen R. Lee of the Blanca Project for their support of this investigation. Much thanks to James R. Kamm and Gary L. Sandine of the Applied Physics Division for assistance in this research.

References

1) Allievi, A. and Bermejo, R., “A Generalized Particle-Search Algorithm for Arbitrary Grids,” *Journal of Computational Physics*, Vol. 132, pp. 157-166, 1997.

2) Lohner, R., “Robust, Vectorized Search Algorithms for Interpolation on Unstructured Grids,” *Journal of Computational Physics*, Vol. 118, pp. 380-387, 1995.

3) Westerman, T., “Localization Schemes in 2D Boundary-Fitted Grids,” *Journal of Computational Physics*, Vol. 101, pp. 307-313, 1992.

4) Lohner, R. and Ambrosiano, J. “A Vectorized Particle Tracer for Unstructured Grids,” *Journal of Computational Physics*, Vol. 91, pp. 22-31, 1990.

5) Wilson, T. L., “LINTERP: A Numerical Algorithm for Interpolating Quadrilateral and Hexahedral Meshes,” Los Alamos National Laboratory Report LA-11902-MS, 1990.

6) Brackbill, J. U. and Ruppel, H. M., “FLIP: A Method for Adaptively Zoned, Particle-in-Cell Calculations of Fluid Flows in Two Dimensions,” *Journal of Computational Physics*, Vol. 65, pp. 314-343, 1986.

7) Pracht, W. E. and Brackbill, J. U., “BAAL: A Code for Calculating Three-Dimensional Fluid Flows at All Speeds with an Eulerian-Lagrangian Computing Mesh,” Los Alamos National Laboratory Report LA-6342, 1976.

8) Brock, J. S., “A Finite-Difference Logical-Coordinate Evaluation Method For Particle Localization,” *Progress of Theoretical Physics*, Sup. 138, pp. 40-42, 2000. (Los Alamos National Laboratory Report LA-UR-99-6493, 1999.)

9) Brock, J. S., “A New Logical-Coordinate Evaluation Method For Particle Localization,” Los Alamos National Laboratory Report LA-UR-99-5355, 1999.

10) Brock, J. S., “Integrating a Bilinear Interpolation Function Across Quadrilateral Cell Boundaries,” Los Alamos National Laboratory Report LA-UR-00-3329, 2000.

Appendix A: Test Problem

The purpose of this appendix is to demonstrate that the five discrete-expansions presented in this report, developed for two-dimensional linear interpolation, are valid across triangular cell boundaries. The following verification has been performed for each expansion in Equations 15, 21, and 27. Within this appendix, however, only one discrete-expansion is used to solve the general problem of two particles located in separate, non-contiguous grid cells. The expansion selected for this demonstration, originally presented in Equation 15, is repeated in Equation A-1.

$$\Delta\overline{X} = \frac{\partial\overline{X}}{\partial\overline{\xi}}(\hat{\overline{X}}^{cv})\,\Delta\overline{\xi} + \frac{\partial\overline{X}}{\partial\overline{X}^{cv}}(\hat{\overline{\xi}})\,\Delta\overline{X}^{cv} \tag{A-1}$$

A particle's state may be defined in two spatial-dimensions as a set of physical-coordinates, $\overline{X} = (x, y)^T$, logical-coordinates, $\overline{\xi} = (\xi, \eta)^T$, and cell-vertex coordinates, $\overline{X}^{cv} = ({}^0\overline{X}, {}^1\overline{X}, {}^2\overline{X})^T$. The only restriction on particle states is that they must form a consistent set of coordinates as described by the interpolation function: $\overline{X} = \overline{X}(\overline{\xi}, \overline{X}^{cv})$. The two particle states used for this demonstration, State 1 and State 2, are defined in Equations A-2 and A-3.

$$\begin{aligned} \text{State 1} \quad : \quad \overline{X}_1 &= (0.2, 0.8)^T \\ \overline{\xi}_1 &= (0.2, 0.4)^T \\ \overline{X}_1^{cv} &= (0, 0, 1, 0, 0, 2)^T \end{aligned} \tag{A-2}$$

$$\begin{aligned} \text{State 2} \quad : \quad \overline{X}_2 &= (1.8, 2.1)^T \\ \overline{\xi}_2 &= (0.1, 0.3)^T \\ \overline{X}_2^{cv} &= (2, 3, 0, 3, 2, 0)^T \end{aligned} \tag{A-3}$$

The discrete-expansion in Equation A-1 includes two first-order interpolation derivatives, $\partial\overline{X}/\partial\overline{\xi}$ and $\partial\overline{X}/\partial\overline{X}^{cv}$. Both transformation matrices are evaluated with average logical-coordinates and average cell-vertex coordinates: $\hat{\overline{\xi}} = (\overline{\xi}_1 + \overline{\xi}_2)/2$ and $\hat{\overline{X}}^{cv} = (\overline{X}_1^{cv} + \overline{X}_2^{cv})/2$. For this demonstration, these average coordinate vectors are presented in Equation A-4.

$$\begin{aligned} \text{State Average} \quad : \quad \hat{\overline{\xi}} &= (\hat{\xi}, \hat{\eta})^T \\ &= (0.15, 0.35)^T \\ \hat{\overline{X}}^{cv} &= ({}^0\hat{x}, {}^0\hat{y}, {}^1\hat{x}, {}^1\hat{y}, {}^2\hat{x}, {}^2\hat{y})^T \\ &= (1, 1.5, 0.5, 1.5, 1, 1)^T \end{aligned} \tag{A-4}$$

The first-order interpolation derivatives in Equation A-1 are scaled by the finite-difference vectors $\Delta\bar{\xi}$ and $\Delta\bar{X}^{cv} = (\Delta^0\bar{X}, \Delta^1\bar{X}, \Delta^2\bar{X})^T$. These vectors are presented in Equation A-5.

$$\begin{aligned} \text{State Delta} \quad : \quad \Delta\bar{X} &= (\Delta x, \Delta y)^T = (1.6, 1.3)^T \\ \Delta\bar{\xi} &= (\Delta\xi, \Delta\eta)^T = (-0.1, -0.1)^T \\ \Delta\bar{X}^{cv} &= (\Delta^0 x, \Delta^0 y, \Delta^1 x, \Delta^1 y, \Delta^2 x, \Delta^2 y)^T \\ &= (2, 3, -1, 3, 2, -2)^T \end{aligned} \tag{A-5}$$

The Jacobian matrix in Equation A-1, $\partial\bar{X}/\partial\bar{\xi}$, was presented in Equation 3 for two-dimensional coordinate transformations. The elements of this matrix were defined in Equation 4. The geometry-transformation matrix, $\partial\bar{X}/\partial\bar{X}^{cv}$, was presented in Equation 5. The product of this matrix and the finite-difference vector $\Delta\bar{X}^{cv}$ is presented in Equation A-6.

$$\frac{\partial\bar{X}}{\partial\bar{X}^{cv}}\,\Delta\bar{X}^{cv} = \frac{\partial\bar{X}}{\partial^0\bar{X}}\,\Delta^0\bar{X} + \frac{\partial\bar{X}}{\partial^1\bar{X}}\,\Delta^1\bar{X} + \frac{\partial\bar{X}}{\partial^2\bar{X}}\,\Delta^2\bar{X} \tag{A-6}$$

As previously noted, the non-square geometry-transformation matrix may be partitioned into diagonal sub-matrices: $\partial\bar{X}/\partial^v\bar{X}$ where $v = 0, 1, 2, 3$. The non-zero elements of each sub-matrix are identical; they are one of the three linear interpolation basis functions. Each sub-matrix may then be defined as an identity matrix scaled by a basis function. The matrix-vector product in Equation A-6 may then be simplified as presented in Equation A-7.

$$\begin{aligned} \frac{\partial\bar{X}}{\partial\bar{X}^{cv}}\,\Delta\bar{X}^{cv} = {} & (1 - \xi - \eta)\,\Delta^0\bar{X} \\ & + (\quad \xi \quad)\,\Delta^1\bar{X} \\ & + (\quad \eta \quad)\,\Delta^2\bar{X} \end{aligned} \tag{A-7}$$

The derivatives and coordinate finite-difference vectors for linear interpolation, required by each discrete-expansion presented in this report, have been defined analytically. The interpolation derivatives were presented as a function of the vectors $\bar{\xi}$ and $\bar{X}^{cv}$. In contrast, the interpolation derivatives in Equation A-1 are evaluated with the average vectors $\hat{\bar{\xi}}$ and $\hat{\bar{X}}^{cv}$. These average coordinate vectors were defined in Equation A-4. The coordinate finite-difference vectors $\Delta\bar{\xi}$ and $\Delta\bar{X}^{cv}$ were defined in Equation A-5. The algebraic form of Equation A-1, including matrices, vectors, scalars, and their products, is presented in Equation A-8.

$$\Delta\bar{X} = \frac{\partial\bar{X}}{\partial\bar{\xi}}(\hat{\bar{X}}^{cv})\,\Delta\bar{\xi} + \frac{\partial\bar{X}}{\partial\bar{X}^{cv}}(\hat{\bar{\xi}})\,\Delta\bar{X}^{cv}$$

$$= \begin{bmatrix} -0.5 & 0 \\ 0 & -0.5 \end{bmatrix}\begin{Bmatrix} -0.1 \\ -0.1 \end{Bmatrix} + (0.5)\begin{Bmatrix} 2 \\ 3 \end{Bmatrix} + (0.15)\begin{Bmatrix} -1 \\ 3 \end{Bmatrix} + (0.35)\begin{Bmatrix} 2 \\ -2 \end{Bmatrix} \qquad \text{(A-8)}$$

$$= (1.6, 1.3)^{T}$$

Equation A-8 correctly predicts the finite-difference in particle physical-coordinates between State 1 and State 2: $\Delta\bar{X} = (1.6, 1.3)^{T}$. Any symmetry or structure exhibited in Equation A-8 is not an inherent feature of discrete-expansions. Instead, these features are an artifact of the test problem. This test problem clearly demonstrates that the five discrete-expansions presented in this report are valid expansions for linear interpolation across triangular cell boundaries.

Figures

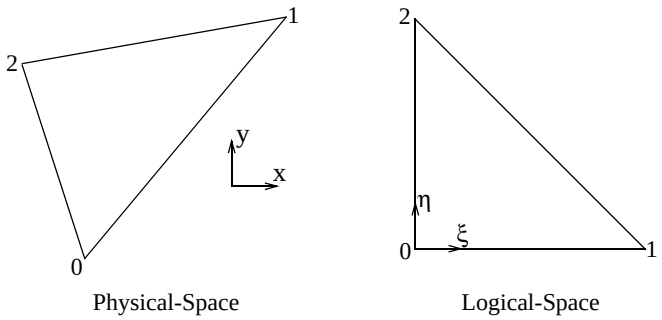

Figure 1: Coordinate Transformation

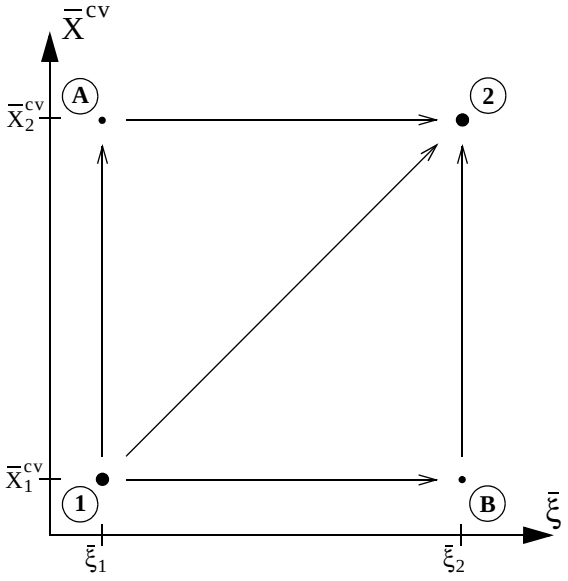

Figure 2: Integration Pathlines